CHAPTER 5 RESULTS AND DISCUSSIONS

This chapter presents the results of the simulation which can be divided into 4 parts. The first part is the results of sensitivity analysis which was performed to find the suitable parameters for tuning the simulation results to match with the experimental data. After validating the model, single-phase results and the comparison between single- and two-phase were studied the direct methanol fuel cell (DMFC) behavior of each parameter. At the end of this chapter, the simulation results of dynamic behavior of DMFC were described.

Table 5.1 provides the experiment conditions and Figure 5.1 shows the experimental data consisting of two variables; cell voltage (V_{cell}) and anode overpotential (η_a).

Table 5.1 The conditions in the experiment

Parameters	Values	Unit
MeOH feed concentration	1000	mol/m^3
Oxygen feed concentration (Air)	9.04	mol/m^3
Cell temperature	90	^oC
Anode catalyst	40 wt% Pt and 20 wt% Ru /C	
Cathode catalyst	60 wt% Pt/C	
Membrane	N-117	

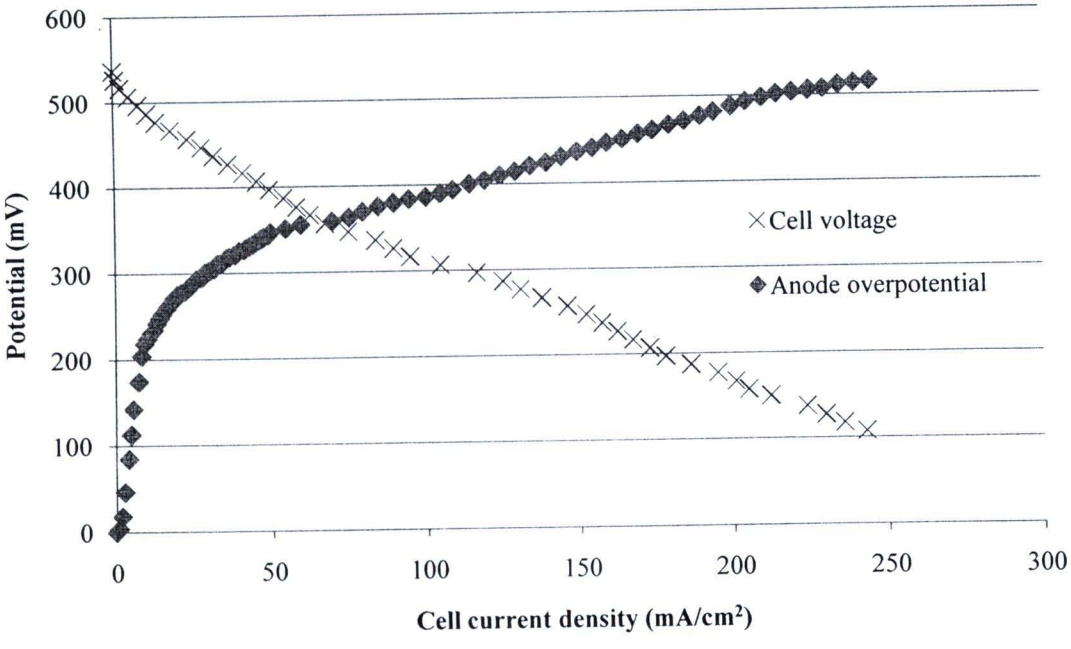

Figure 5.1 The in-house experiment data

5.1 Sensitivity Analysis and Validation

From Equation 4.11, the cell voltage depends on three values; anode and cathode overpotentials (η_a and η_c) and ohmic overpotential. In this step, the parameters affecting these three overpotentials were varied to find the suitable values. For the anode overpotential, the reaction rate constants for anode reaction in steps 1 and 2 (k_{a1}, k_{a2}) and transfer coefficients of anode reaction in steps 1 and 2 (α_{a1}, α_{a2}) were adjusted while the transfer coefficient of cathode reaction (α_c) and cathode exchange current density (j^{ref}_{0,O_2}) were adjusted to investigate the effect of cathode overpotential on the cell voltage. Moreover, the ohmic contact resistance ($R_{contact}$) was also adjusted to investigate the ohmic loss. Thus, all parameters were individually varied to observe theirs trend. Except for the transfer coefficients of anode reaction, the parameters were varied simultaneously at the same value. Table 5.2 shows the values of each parameter which were used as the base-case. When varying one parameter, the other parameters were fixed as the constants which were the base-case values. The results after varying these parameters are shown below.

Table 5.2 The values of parameters in the base-case

Parameters	Symbols	Value	Unit
Reaction rate constant of anode reaction			
step 1	k_{a1}	1.6×10^{-3}	mol m^{-2} s^{-1}
step 2	k_{a2}	8.0×10^{-5}	mol m^{-2} s^{-1}
Transfer coefficient of anode reaction			
step 1&2	α_{a1}, α_{a2}	0.5	-
Transfer coefficient of cathode reaction			
	α_c	1.0	-
Cathode exchange current density	j^{ref}_{0,O_2}	1.14×10^{3}	A m^{-3}
Ohmic contact resistance	$R_{contact}$	0.0	Ω m^2

5.1.1 Anode Overpotential

In this model, anode overpotential consisted of activation and concentration losses since the resistance from mass transport of methanol in the diffusion layer and catalyst layer had been already considered.

- Reaction rate constants for anode reaction

Figures 5.2 and 5.3 demonstrate that when the reaction rate constants decreased, the anode overpotentials would increased. This was because the reduction in the rate constants led to a slower rate of reaction. The electrons which produced in this reaction were not enough for producing cell current density. Therefore, the cell tried to produce the current density by increasing the anode overpotential.

In addition to these figures, the values of reaction rate constants for anode reaction affected the anode overpotential differently. The variation of both reaction rate constants for anode reaction affected the onset potential but the variation of reaction rate constant for anode reaction step 1 had a significant effect upon the Tafel slope of the reaction.

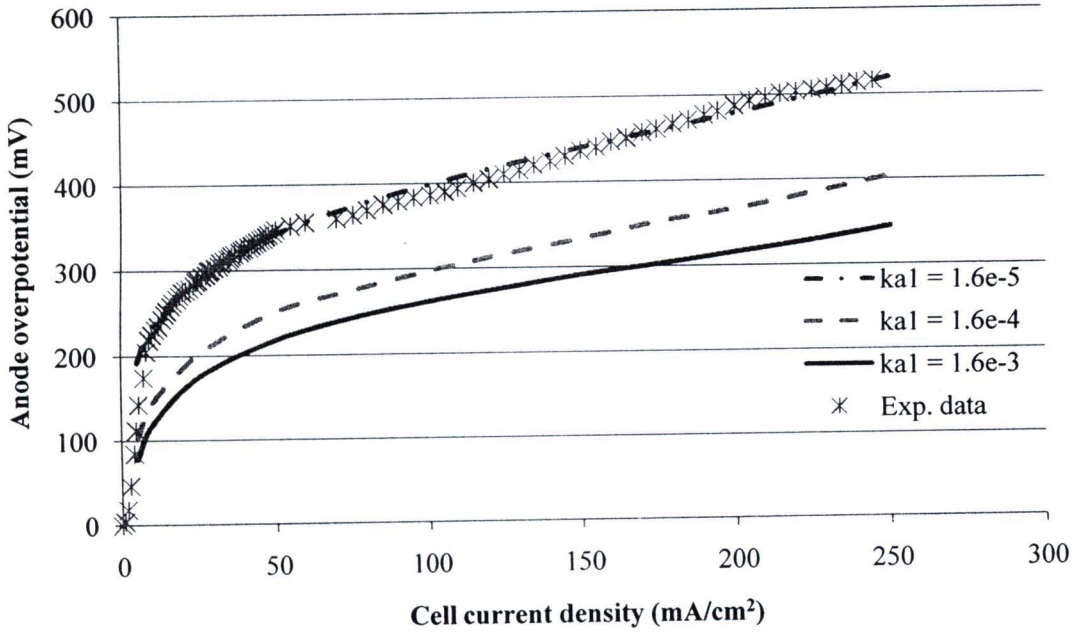

Figure 5.2 Effects of reaction rate constant of the anode reaction step 1 (k_{a1}) and cell current density on the anode overpotential (η_a)

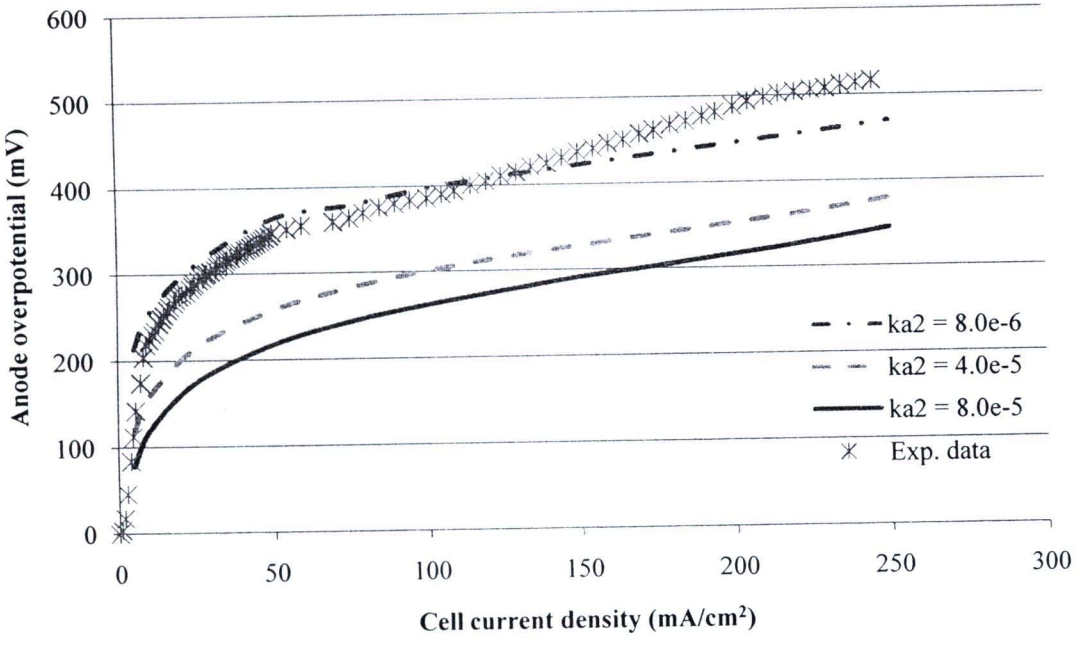

Figure 5.3 Effects of reaction rate constant of the anode reaction step 2 (k_{a2}) and cell current density on the anode overpotential (η_a)

- Transfer coefficient of anode reaction

From Figure 5.4, the transfer coefficients of anode reaction steps 1 and 2 affected the Tafel slope which was similar to the reaction rate constant of anode reaction step 1.

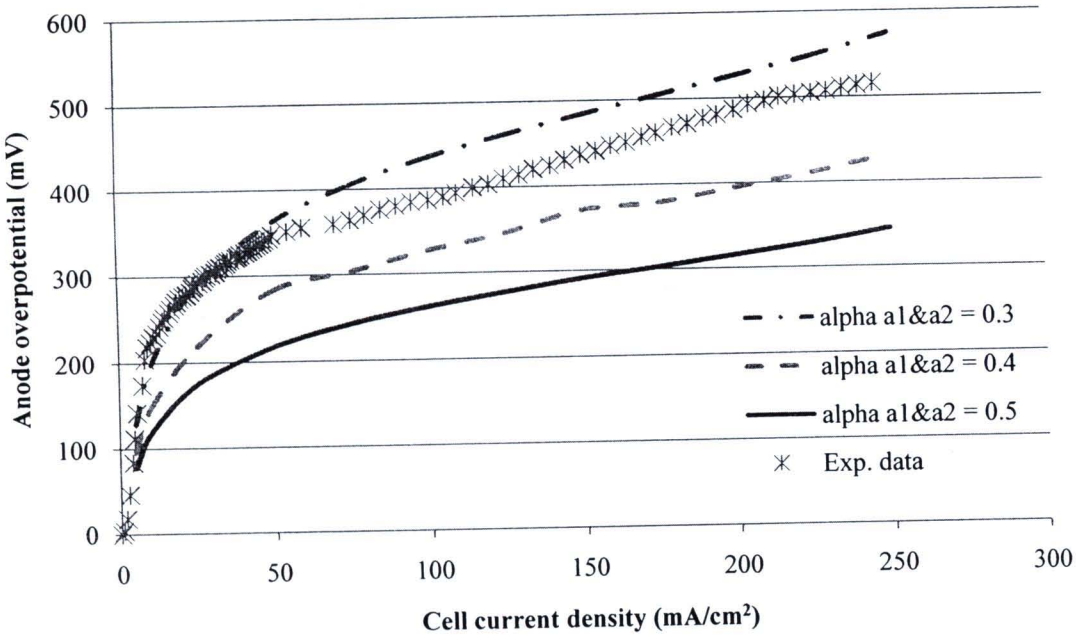

Figure 5.4 Effects of transfer coefficient of the anode reaction steps 1 and 2 (α_{a1}, α_{a2}) and cell current density on the anode overpotential (η_a)

5.1.2 Cathode Overpotential

Because of the lack of the experimental data of the cathode overpotential to validate the simulation model prediction, the simulation results which used to compare were the cell voltage. For cathode overpotential, there were only two studied parameters which were the transfer coefficient of cathode reaction and cathode exchange current density. The comparison of the cell voltage obtained from the experimental data and simulation results are presented in Figures 5.5 and 5.6.

- Transfer coefficient of cathode reaction

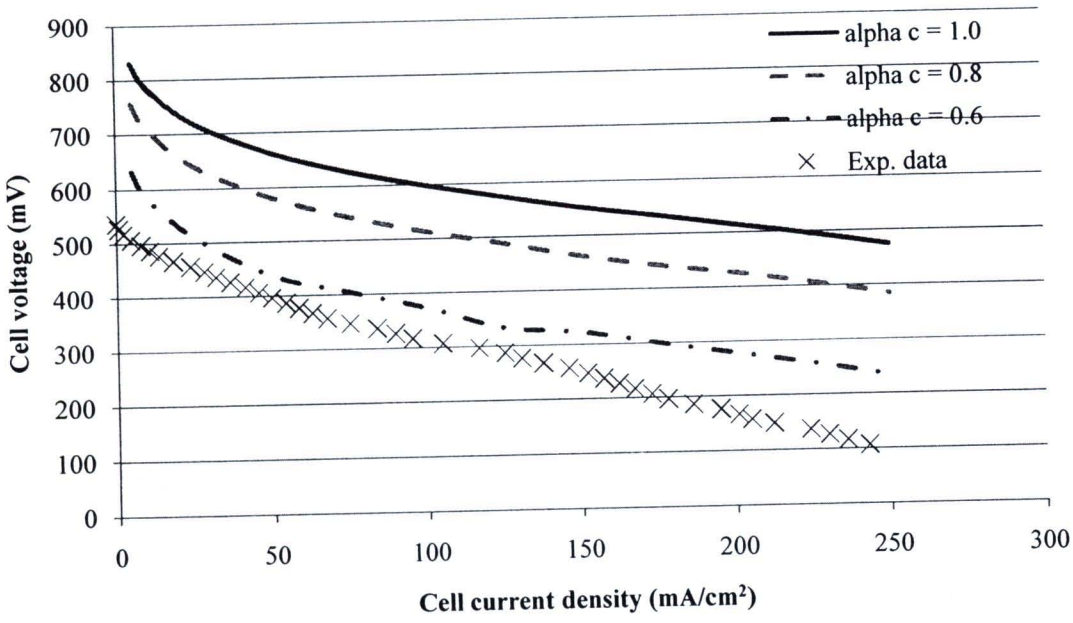

Figure 5.5 Effects of transfer coefficient of the cathode reaction (α_c) and cell current density on the cathode overpotential (η_c)

- Cathode exchange current density

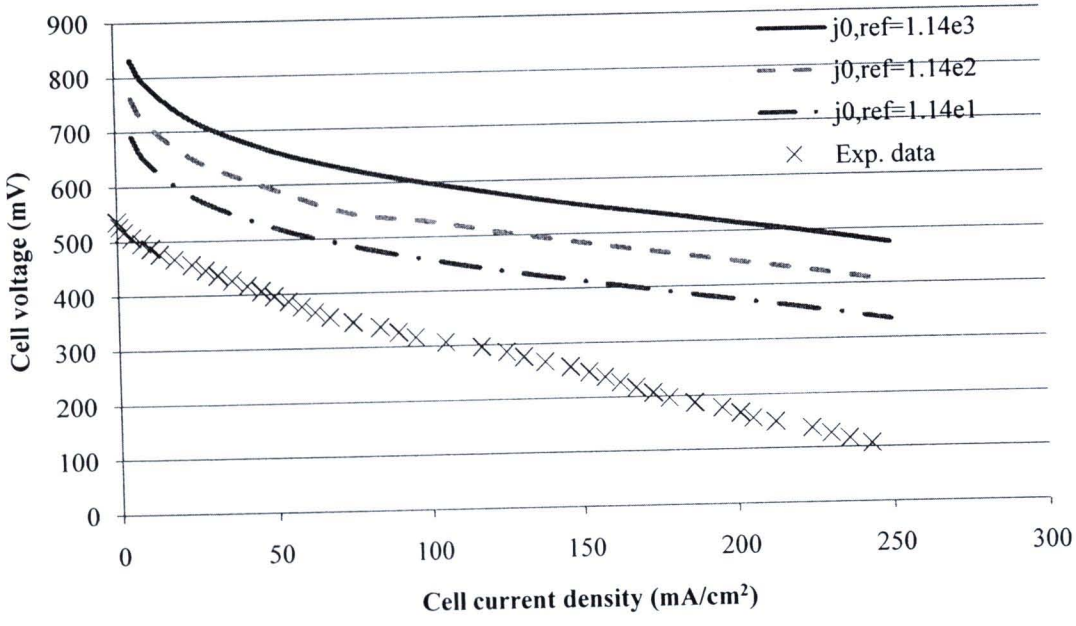

Figure 5.6 Effects of cathode exchange current density (j_{0,O_2}^{ref}) and cell current density on the cathode overpotential (η_c)

From Figures 5.5 and 5.6, both the transfer coefficient of the cathode reaction and the cathode exchange current density affect the cell voltage but the trends are different. When the transfer coefficient of the cathode reaction decreased, the cell voltage was decreased. While the cathode exchange current density increased the cell voltage was decreased.

5.1.3 Ohmic Contact Resistance

Ohmic contact resistance ($R_{contact}$) was the last parameter which was considered. It affected the ohmic overpotential which was that when the current density increased, the ohmic overpotential increased. From Figure 5.7, the slope of the cell voltage was increased when the ohmic contact resistance increased.

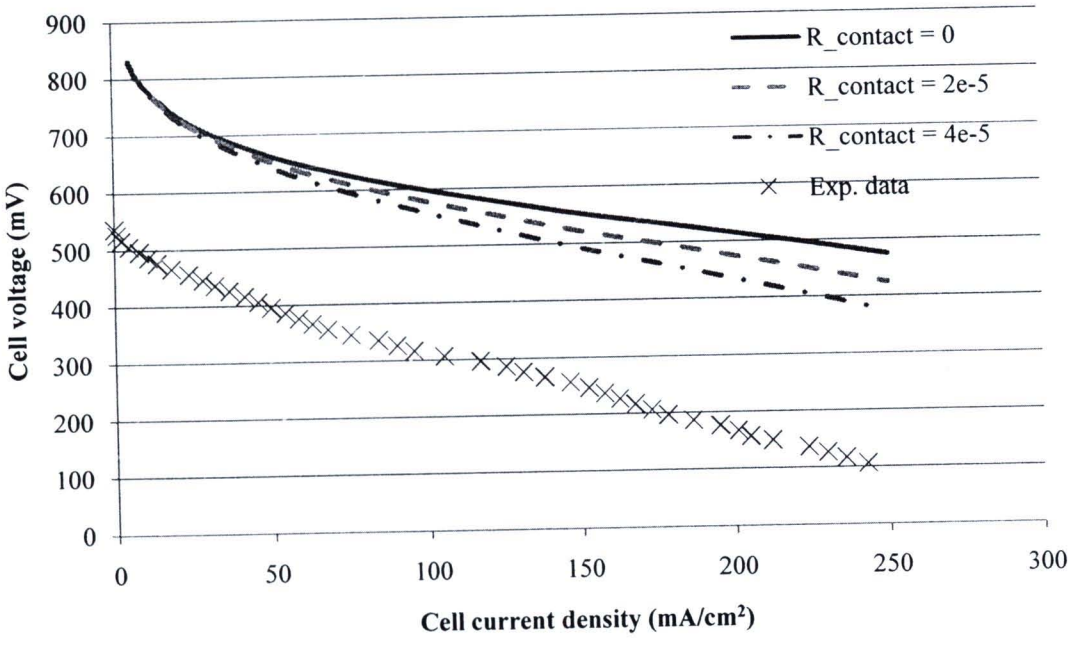

Figure 5.7 The cell voltage predicted by the model with varying the value of $R_{contact}$

5.1.4 Validation of Anode Overpotential and Cell Voltage

From the sensitivity analysis, the parameters which are suitable for tuning the model are the reaction rate constants for anode reaction, cathode exchange current density and ohmic contact resistance.

Since the values of the base-case were from the literature in which its experimental conditions and the membrane electrode assembly were different, then the value of each parameter was changed to fit the model. After the simulation result fitted with the experimental data, the results are shown in Figures 5.8 and 5.9 and the value of parameters found are shown in Table 5.3.

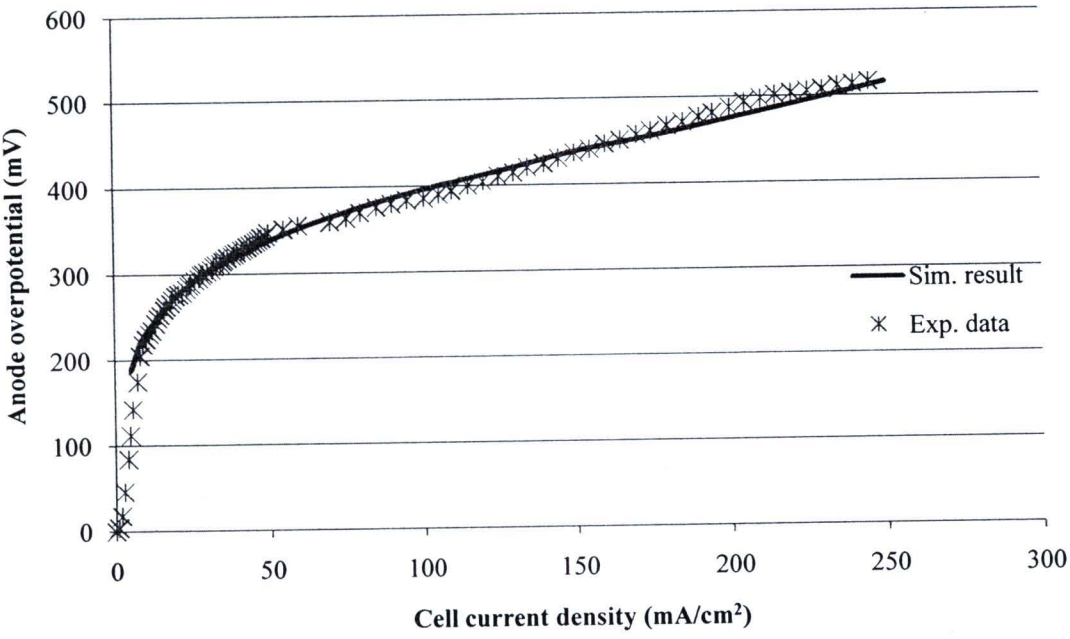

Figure 5.8 The comparison of anode overpotential curves between the modeling and the experimental data

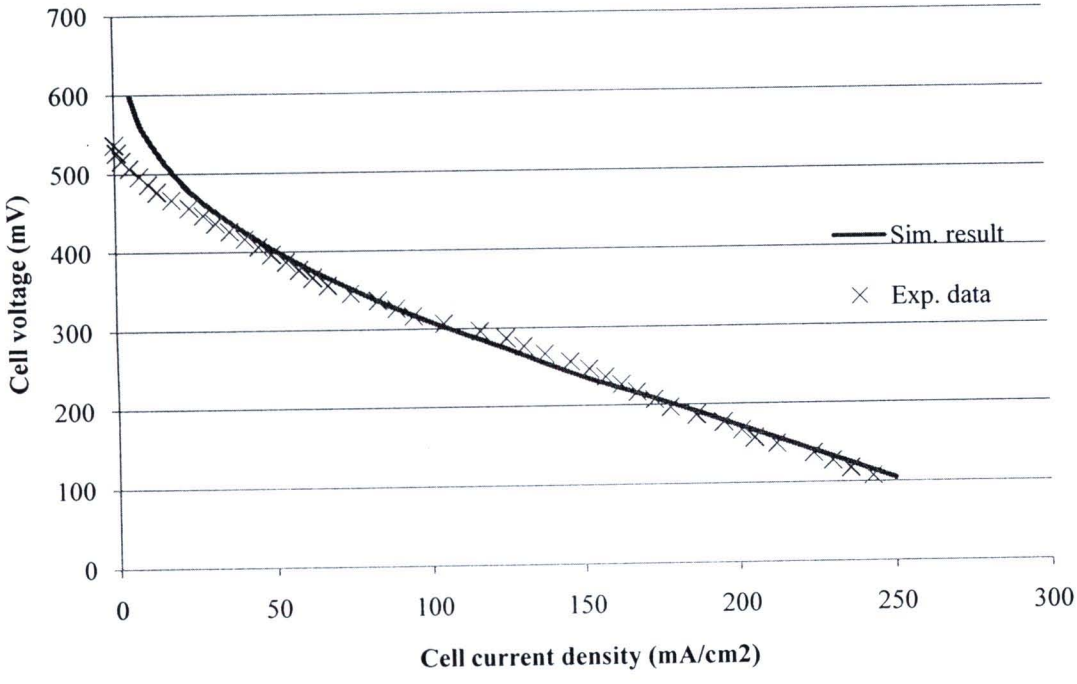

Figure 5.9 The comparison of voltage cell polarization curves between the modeling and the experimental data

Table 5.3 Parameters used in the mathematical model

Parameters	Symbols	Unit	Model value	Literature value
Reaction rate constant of anode reaction				
step 1	k_{a1}	mol m^{-2} s^{-1}	1.7×10^{-5}	1.6×10^{-3}
step 2	k_{a2}	mol m^{-2} s^{-1}	9.0×10^{-5}	8.0×10^{-5}
Cathode exchange current density				
	j^{ref}_{0,O_2}	A m^{-3}	20	1.14×10^{3}
Ohmic contact resistance				
	$R_{contact}$	Ω m^2	3.0×10^{-5}	0.0

5.2 Steady-State Behavior of DMFC

After the simulation results were validated with experimental data, the other parameters were studied, such as all polarizations, liquid saturations of anode and cathode side, and methanol liquid and oxygen concentrations, by varying the current density.

Figure 5.10 shows the cell voltage and individaul overpotentials. The anode overpotential had low value in the initial and continuously increased with the current density. In contrast to the anode overpotential curve, the cathode overpotential was initially high. As the current density increased, the cathode overpotential was slightly increased when comparing with the anode overpotential. Finally, it was observed that the ohmic overpotential was not significant because the proton conductivity was high.

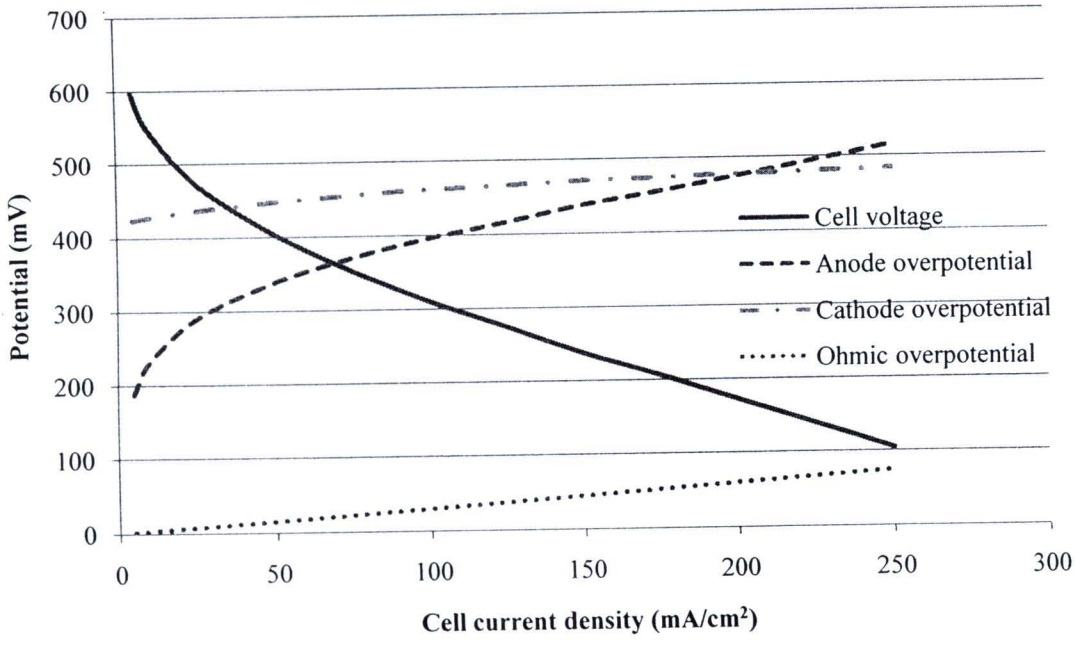

Figure 5.10 All polarization losses and cell voltage

Figures 5.11-5.13 show the anode and cathode liquid saturation, the methanol concentration and oxygen concentration which plot with the thickness of fuel cell for variation of the cell current density.

From Figure 5.11, the liquid saturation in the anode diffusion layer was higher than in the anode catalyst layer because carbon dioxide was generated in the catalyst layer and then was transferred from the catalyst layer to the flow channel. In contrast to the saturation in the anode side, the liquid saturation in the cathode catalyst layer was higher than in the cathode diffusion layer since water was generated in the catalyst layer and was transferred by capillary force to the flow channel. It can be understood that the carbon dioxide and water generation in the catalyst layer related closely to current density. Thus, a higher current density yields more carbon dioxide and water, and results in a lower liquid saturation value in the anode side and a higher liquid saturation value in the cathode side.

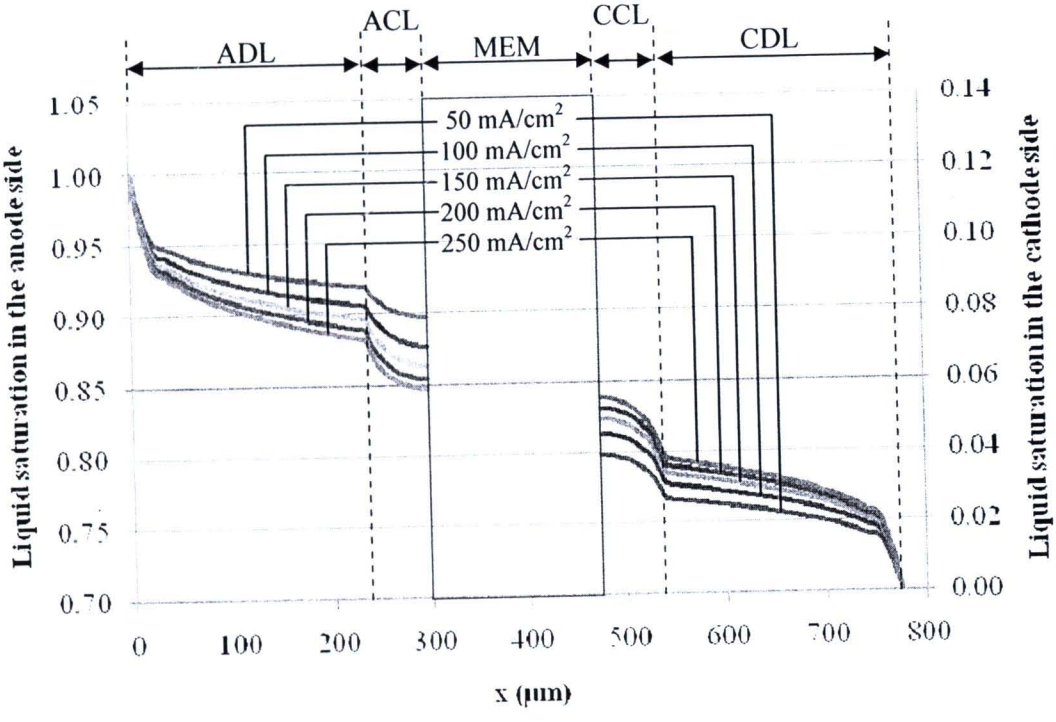

Figure 5.11 The liquid saturation of anode and cathode side at various cell current densities

Figure 5.12 shows the methanol concentration at the middle of channel. The methanol concentration is highest at the inlet and the concentration decreases sharply. In the catalyst layer, the concentration is steeper decreased since the methanol is consumed. Furthermore, the concentration of methanol reaches zero at the membrane-cathode catalyst layer interface since the methanol which crossover through the membrane is completely consumed at the cathode catalyst layer.

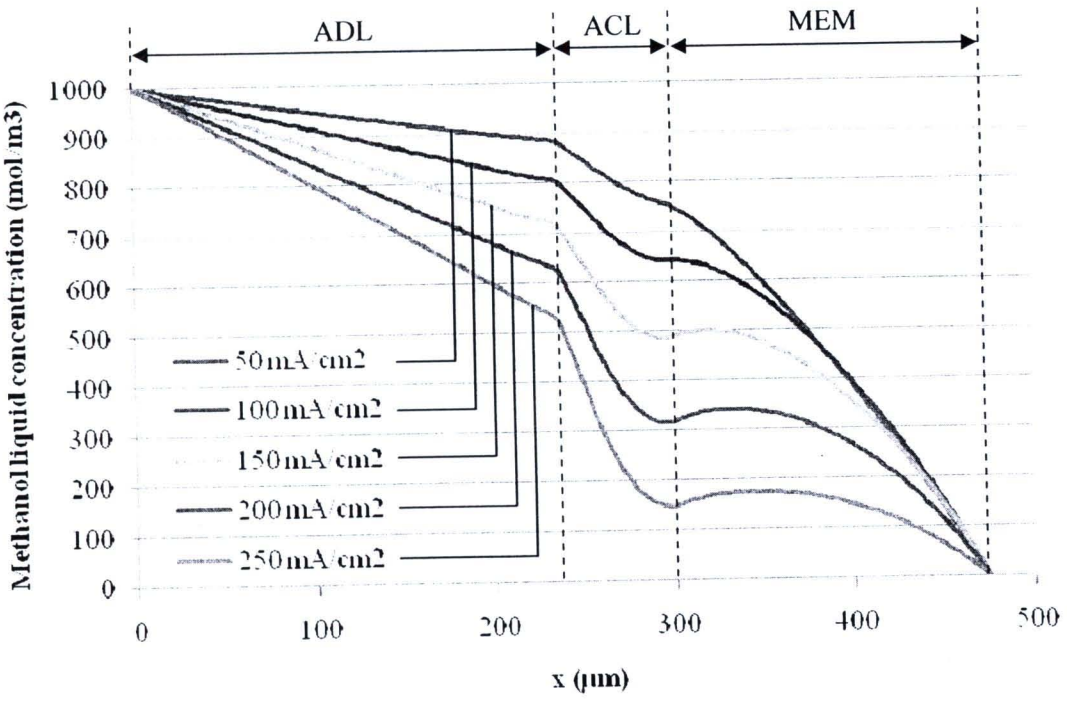

Figure 5.12 The methanol liquid concentration at various cell current densities

The distribution of oxygen concentration in the cathode side is show in Figure 5.13. Oxygen transfers through the diffusion layer to the catalyst layer. Due to the consumption of oxygen by ORR, the oxygen concentration becomes lower in the catalyst in the catalyst layer. However the decrease of oxygen concentration form the channel to catalyst layer is much smaller because of the rather low transport resistance of oxygen in the gas phase.

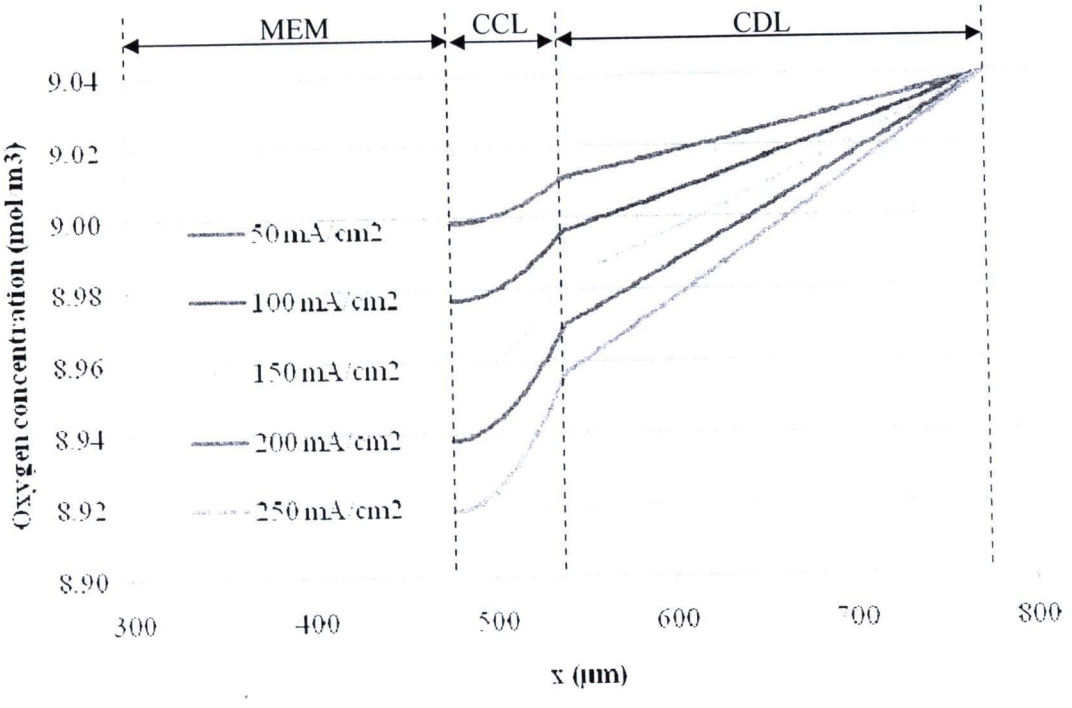

Figure 5.13 The oxygen concentration at various cell current densities

5.3 Comparing Single- and Two-phase Models

In this section, the polarization curves predicted by two-phase model are compared with those predicted by other models. Figure 5.14 shows the polarization curve of each model which is explained below.

1. Case A shows the cell voltage of two-phase model in which both the liquid and vapor phase mass transport of methanol and the effect of non-equilibrium evaporation and condensation were considered.
2. Case B corresponds to the model in which the mass transports of liquid methanol and carbon dioxide are considered, but methanol and water vapor in the gas phase are ignored.
3. Case C represents the simulation result of the single-phase model in which insignificance of the blockage of carbon dioxide is assumed.
4. Case D represents the model in which the anode liquid saturation is a constant value (0.8) and the methanol and water in gas phase, and carbon dioxide are considered.

For all the models, the difference between each model is distinguished by the Eq. 4.15 whereby the anode liquid saturation and the source term in this equation were calculated. For both cases A and B, the two-phase mass transport in which the liquid saturation of the anode side was calculated from Eq. 4.15 was considered. However, a difference between cases A and B which is the source term. The source term of case A in the anode catalyst layer included the generated carbon dioxide and the phase change of both water and methanol as shown in Eq. 4.36. While that of case B only generated carbon dioxide was considered. It means that water and methanol were in liquid phase only. Moreover, in the model of cases C and D Eq. 4.15 was ignored, and the constant liquid saturation was assumed.

From Figure 5.14, it can be observed that the cell voltage of each model is different at high cell current density and the cell voltage of case D is mostly different from another. Moreover, from Figure 5.15, the anode overpotentials for all cases are represent in the range of high cell current density which corresponds to the cell voltage, while the difference of cathode overpotentials among different cases as shown in Figure 5.16 is not significant.

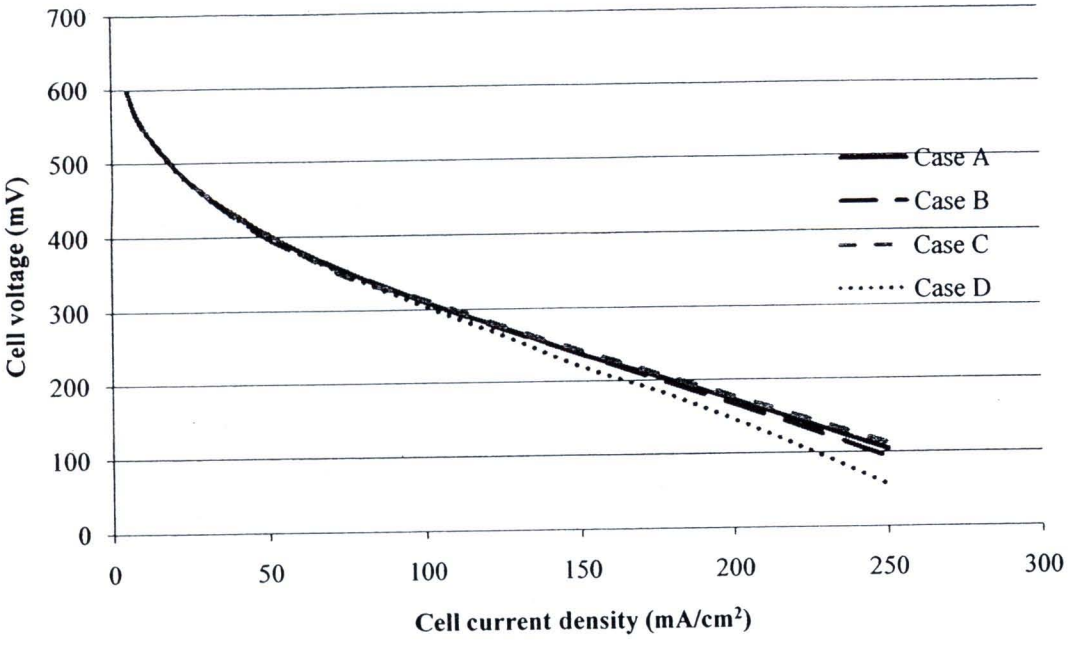

Figure 5.14 Polarization curves predicted by different models

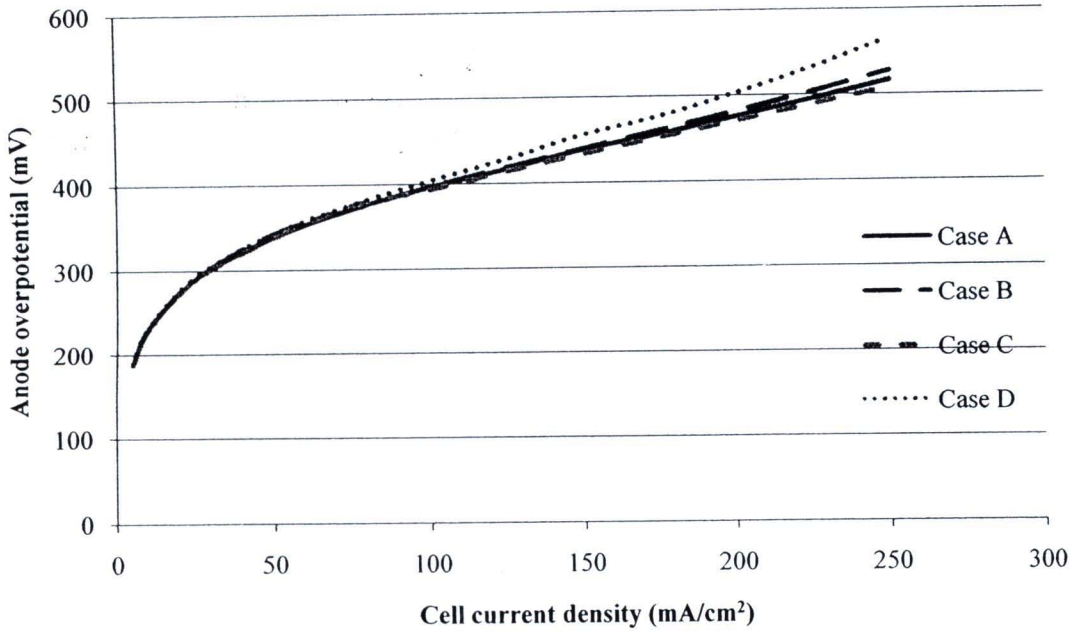

Figure 5.15 Anode overpotentials predicted by different models

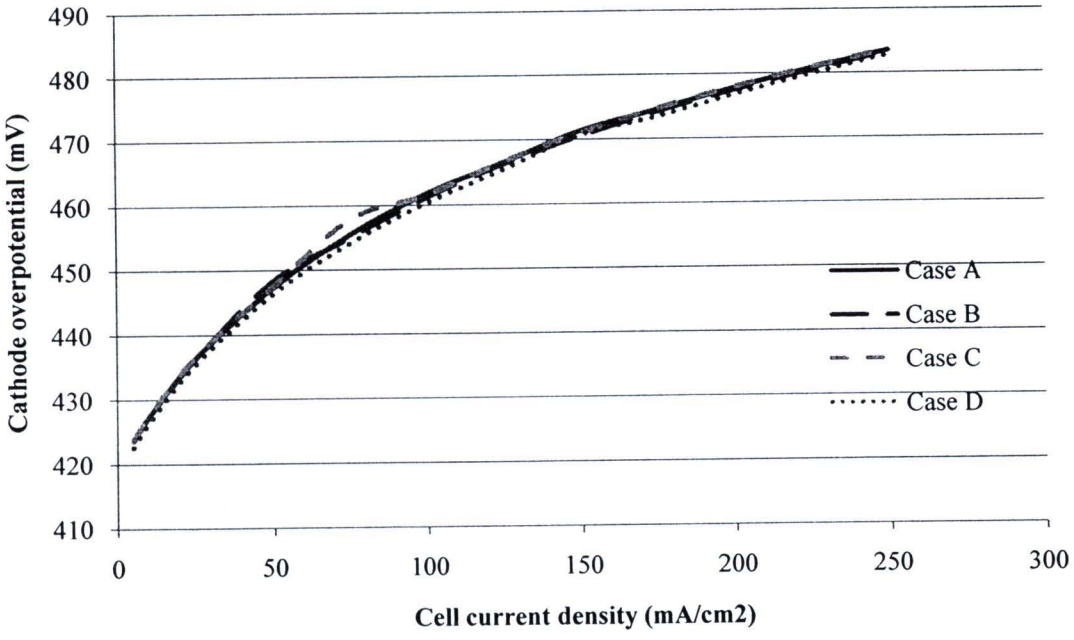

Figure 5.16 Cathode overpotentials predicted by different models

Figures 5.17 and 5.18 show the liquid saturation and methanol concentration in ACL, respectively. Form these figures, when the liquid saturation was high the methanol concentration in ACL was also high. It is imply that the liquid saturation affects the mass transport of methanol in anode region causing the change of methanol the concentration in ACL. Then, when the concentration of methanol is low, the anode overpotential will increase to keep the current production. Consequently, the anode overpotential result also affects cell voltage.

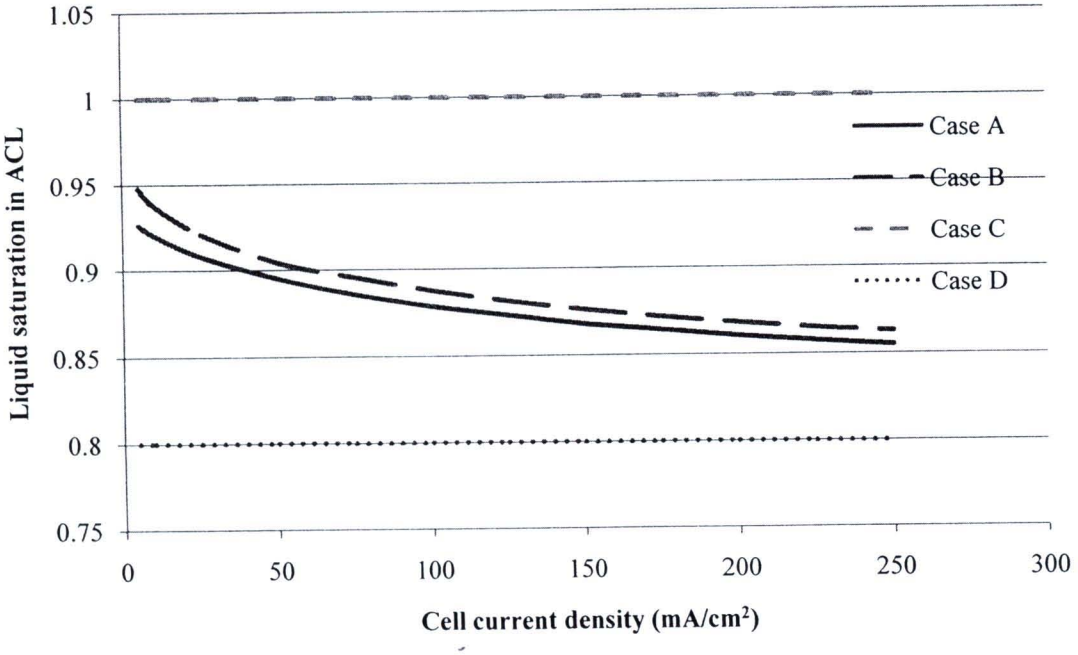

Figure 5.17 Liquid saturation in ACL predicted by different model

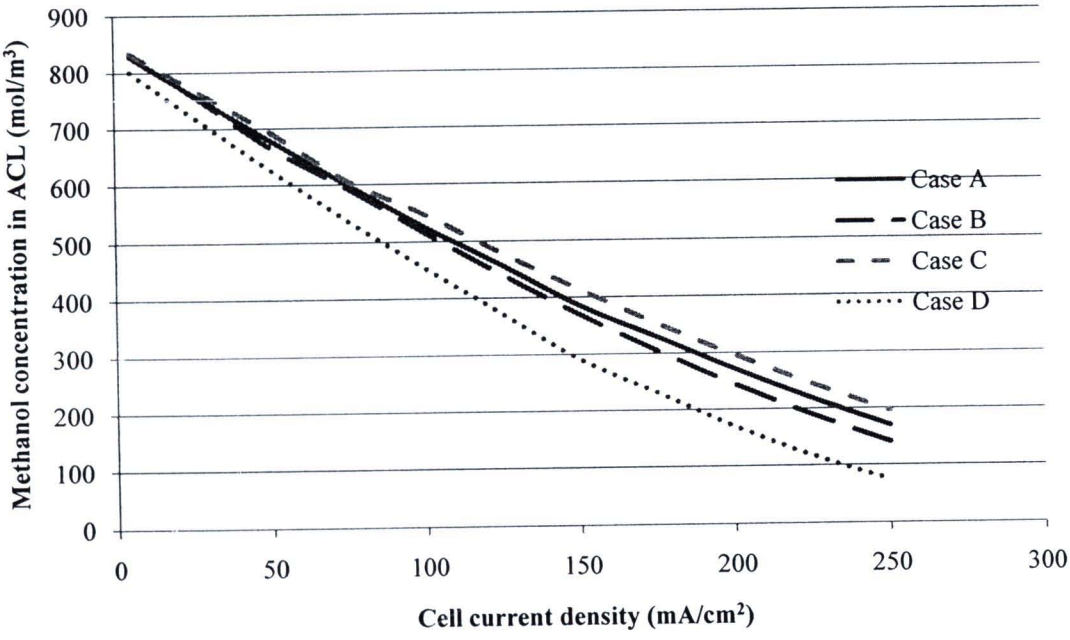

Figure 5.18 Methanol concentration in ACL predicted by different model

5.4 Dynamic Behavior of DMFC

In this topic, the dynamic behavior which responded to the step changes in current density was discussed. There are 9 studied parameters which are cell voltage, anode and cathode overpotential, liquid saturation in ACL and CCL, methanol and oxygen concentration, averaged CO coverage, and parasitic current density. The dynamic simulation results have 3 cases which are different in the step-change of current density; 1) 200 to 50 mA/cm^2 2) 200 to 100 mA/cm^2, and 3) 200 to 150 mA/cm^2.

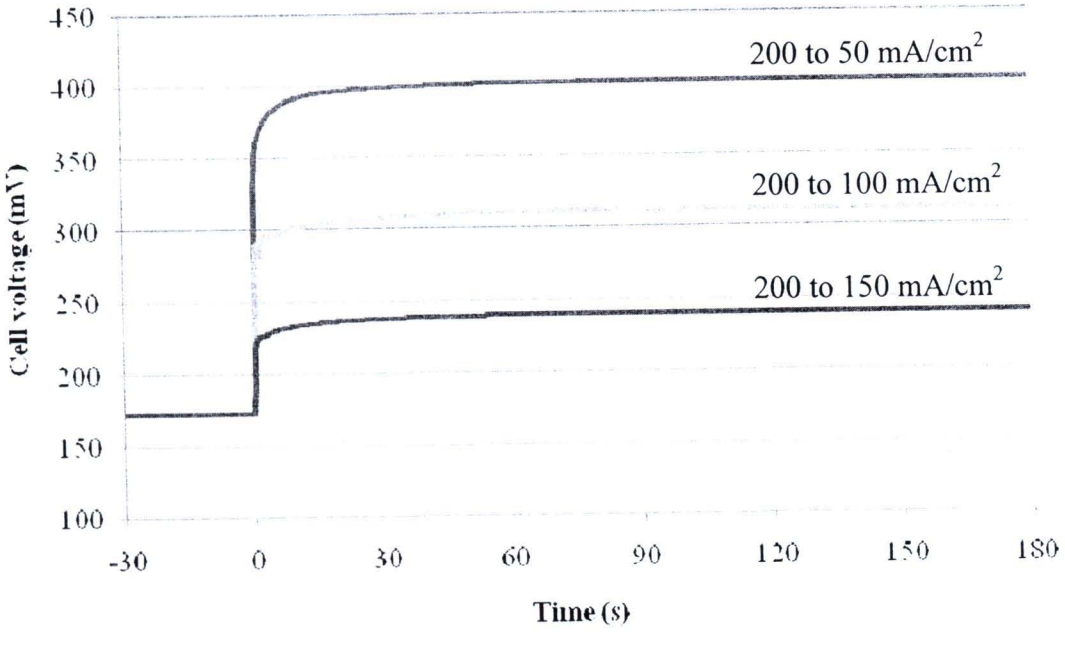

Figure 5.19 Dynamic behavior of the cell voltage

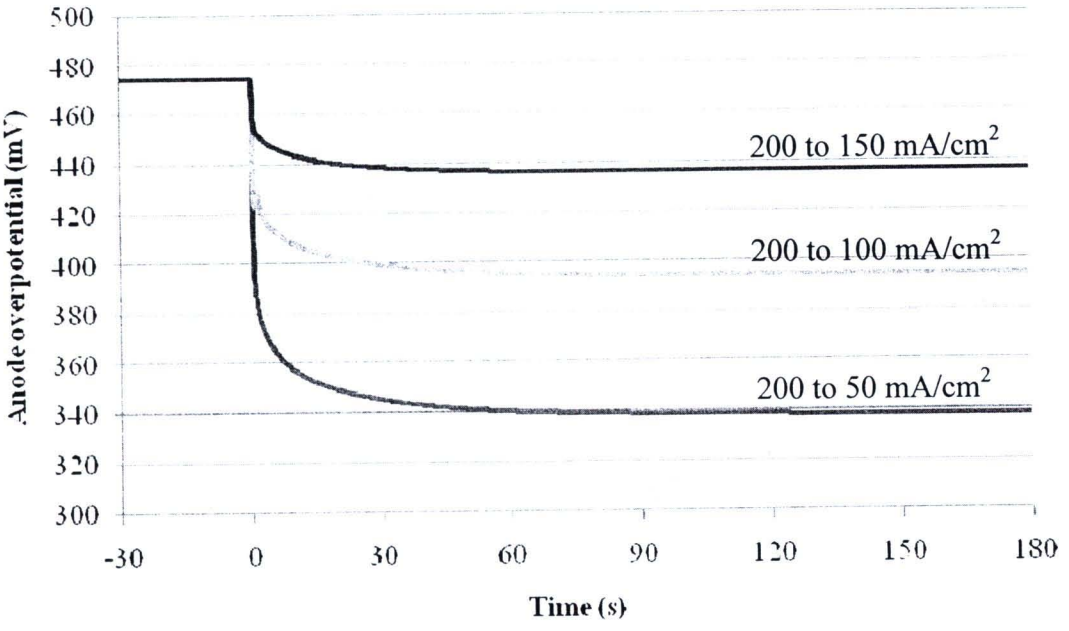

Figure 5.20 Dynamic behavior of the anode overpotential

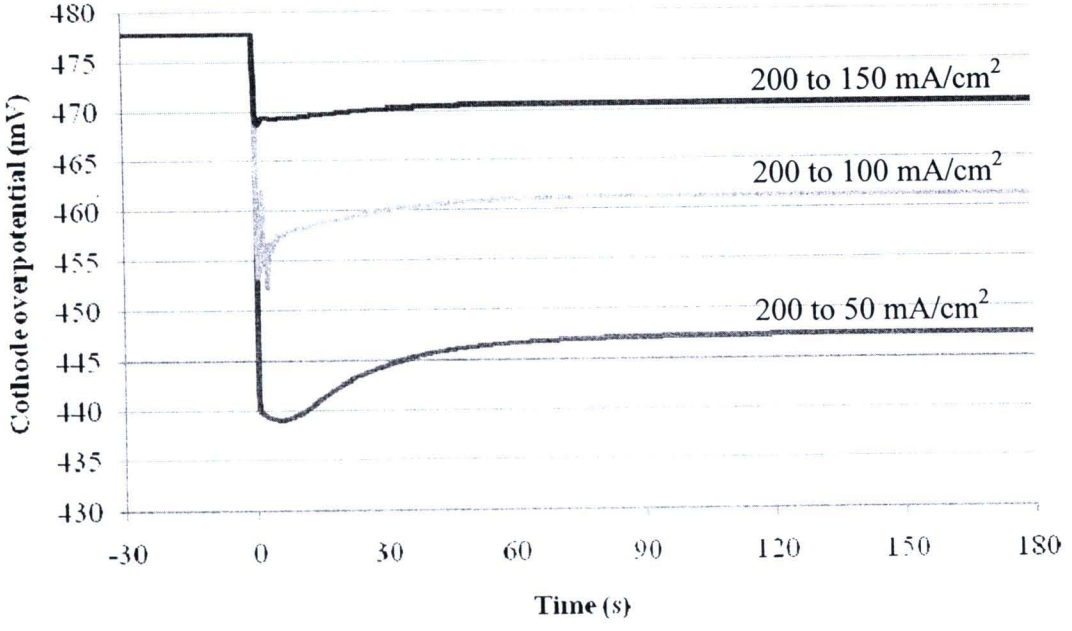

Figure 5.21 Dynamic behavior of the cathode overpotential

The dynamic behavior of cell voltage is shown in Figure 5.19. From this figure, the cell voltage suddenly changes to a higher value and slightly increases until it reaches a new steady-state. The whole process took over 70 s to reach a stable value. Moreover, the anode and cathode overpotentials were studied and plotted in Figures 5.20 and 5.21 in order to study the factor that causes the dynamic behavior of the cell voltage.

For all cases, the anode overpotential suddenly drops and slightly decreases to a stable value. While the cathode overpotential sharply drops to a lower value and gradually increases to a stable value. As can be seen, the undershoot behaviors of cathode overpotential correspond to the decrease in the current density. Both anode and cathode overpotentials take over 70 s to reach the new steady-state.

For the case that the current density drops from 200 to 50 mA/cm^2, the magnitude of the cathode overpotential undershooting is about 9 mV. While for, the anode overpotential the difference between the value initially drops and a new steady-state value is reached about 50 mV. It can be seen that the difference of the anode overpotential is higher than the magnitude of the cathode overpotential undershooting. Then, the cell voltage does not present the overshooting even if the cathode overpotential occurs the undershooting. To explain the behaviors of the anode and cathode overpotentials, the physicochemical process were discussed next.

The dynamic behavior of CO coverage was studied because it was known as catalyst poisoning which related to the kinetics and affected the performance of the fuel cell. Figure 5.22 shows the dynamic behavior of CO coverage in response to the changes in cell current density. The CO coverage had low value which was about 0.05 to 0.12 and it had higher value when the current density was low. Since Pt catalyst sites were more than needed for the complete methanol oxidation, methanol adsorption and the dehydrogenation step became prevailing when the current density changed [15]. Then, in a suddenly drop of the current density, the CO coverage slightly changed. Moreover, it took approximately 90 s to reach a new steady state.

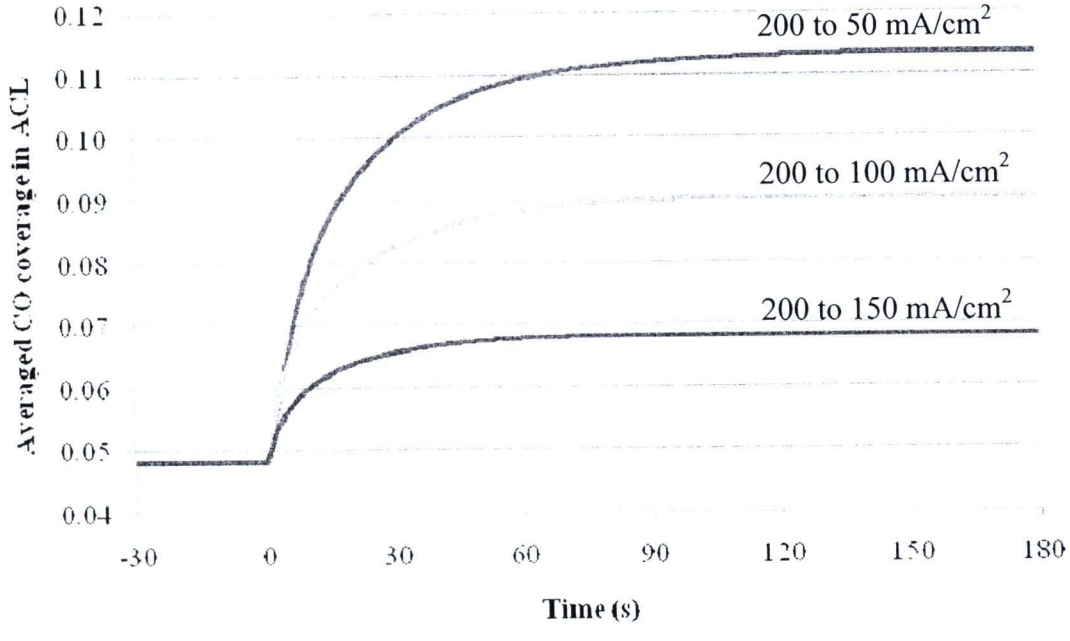

Figure 5.22 Dynamic behavior of the average CO coverage in ACL

Figures 5.23 and 5.24 show the liquid saturation and methanol concentration in ACL. As can be seen, after changing the current density, the liquid saturation sharply increased and presented the overshoot behavior. When the current density suddenly droped, the generated carbon dioxide was smaller and then the liquid saturation in the ACL was decreased. Moreover, Figure 5.24 shows the methanol concentration in ACL. The methanol concentration in ACL is the important parameter that may influence the kinetics of the anode electrode reaction. As can be seen, the sudden decrease of the current density affected the methanol concentration since the demand of methanol for electro-oxidation decreased. Therefore, the methanol began to accumulate until it reached the new steady-state value which took over 90 s. Although the methanol concentration was greatly changed, it did not show a significant influence on the anode overpotential. It can be explained that the kinetics of the anodic MOR is insensitive to methanol concentration.

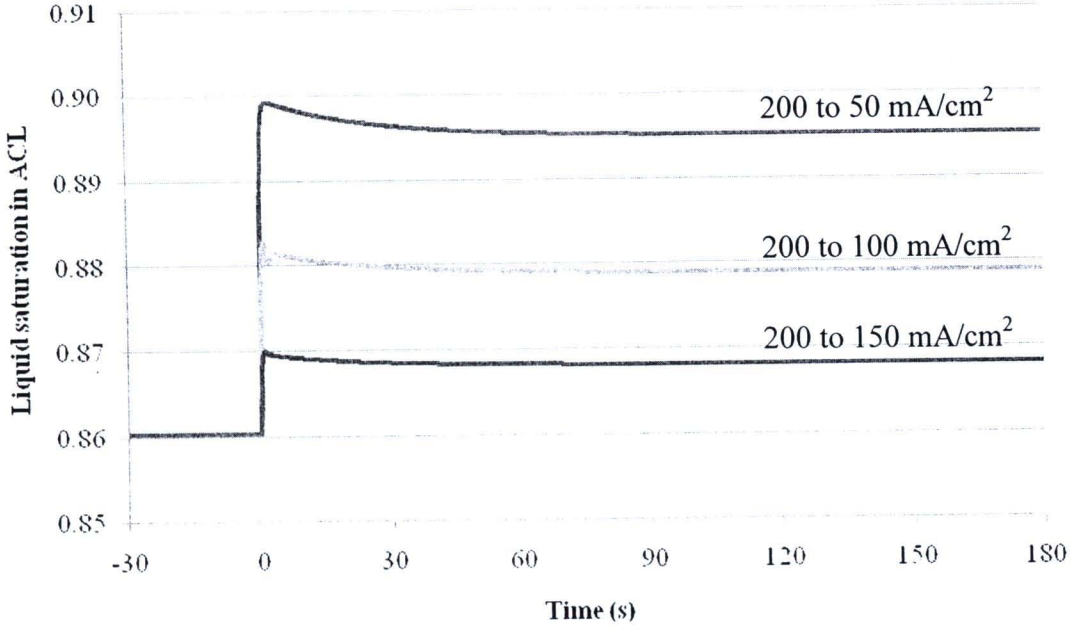

Figure 5.23 Dynamic behavior of the average liquid saturation in ACL

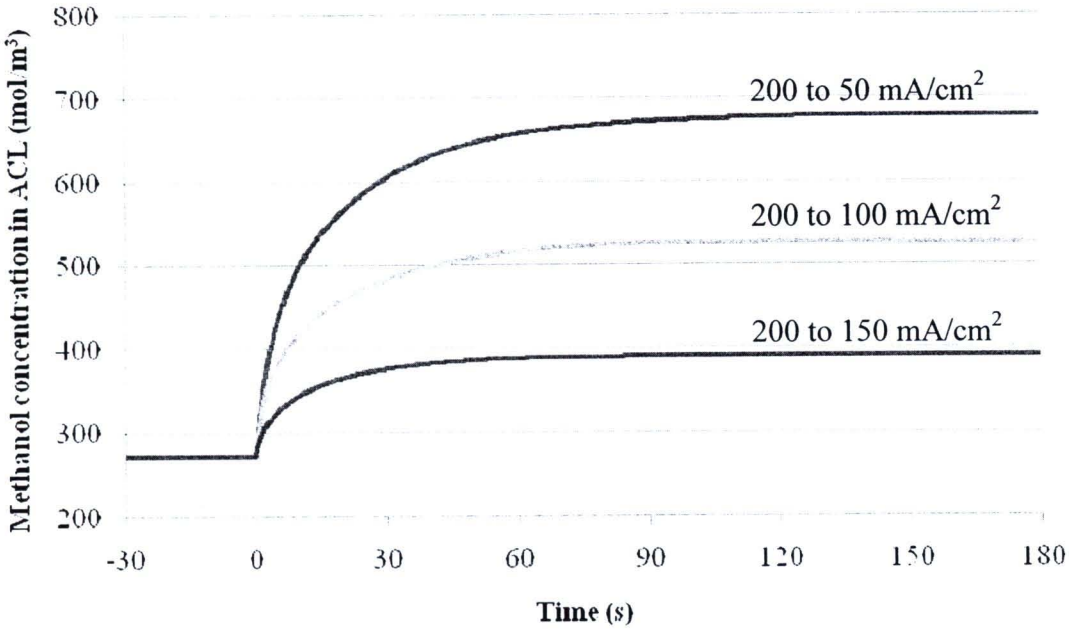

Figure 5.24 Dynamic behavior of the average methanol concentration in ACL

Furthermore, the methanol concentration in ACL also affected the parasitic current density which is shown in Figure 5.25. The parasitic current density expresses the flux of methanol crossover through the membrane. When the current density was changed, the flux of methanol crossover increased and the behavior of methanol crossover were obviously in the same time range as the methanol concentration increased.

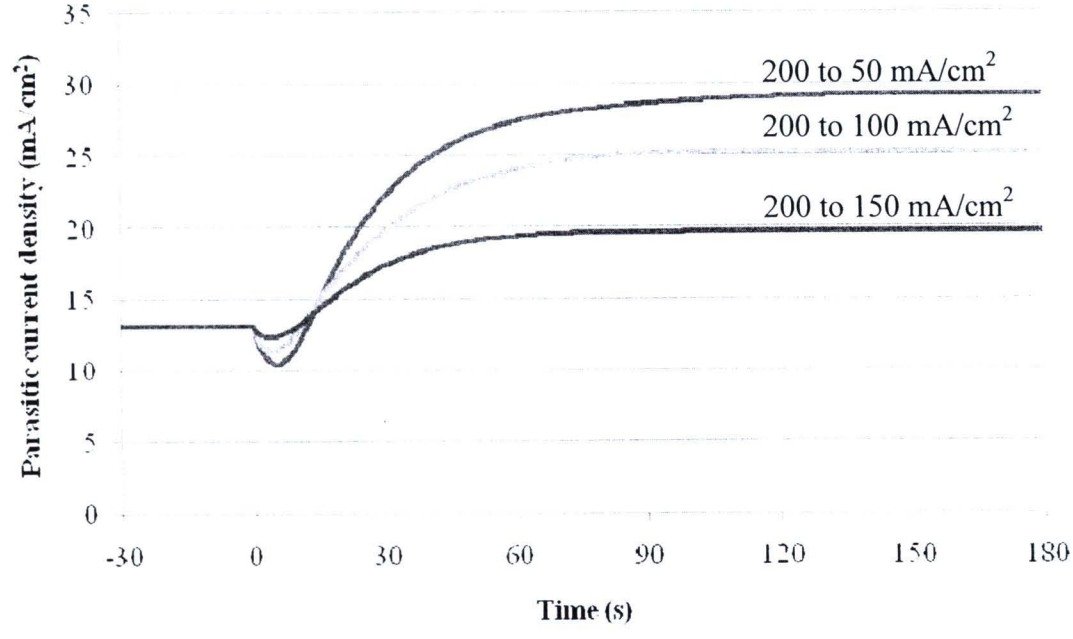

Figure 5.25 Dynamic behavior of the parasitic current density

Figures 5.26 and 5.27 show the dynamic behaviors of liquid saturation and oxygen concentration in CCL which may affect the cathode overpotential. From the figure, the liquid saturation in CCL slowly decreased until it reached a new steady-state while the oxygen concentration increased to a higher value, and then it slowly decreased until it reached a new steady-state. As it can be seen, the behavior of oxygen concentration corresponded to that of the cathode overpotential. When the current density was step change, the concentration of oxygen showed the overshooting and it took over 70 s while the cathode overpotential present undershoot behavior and it also took over 70 s. Therefore, the oxygen concentration was the main factor which resulted in the undershooting of cathode overpotential. Moreover, the parasitic current density was also a factor that affected the cathode overpotential.

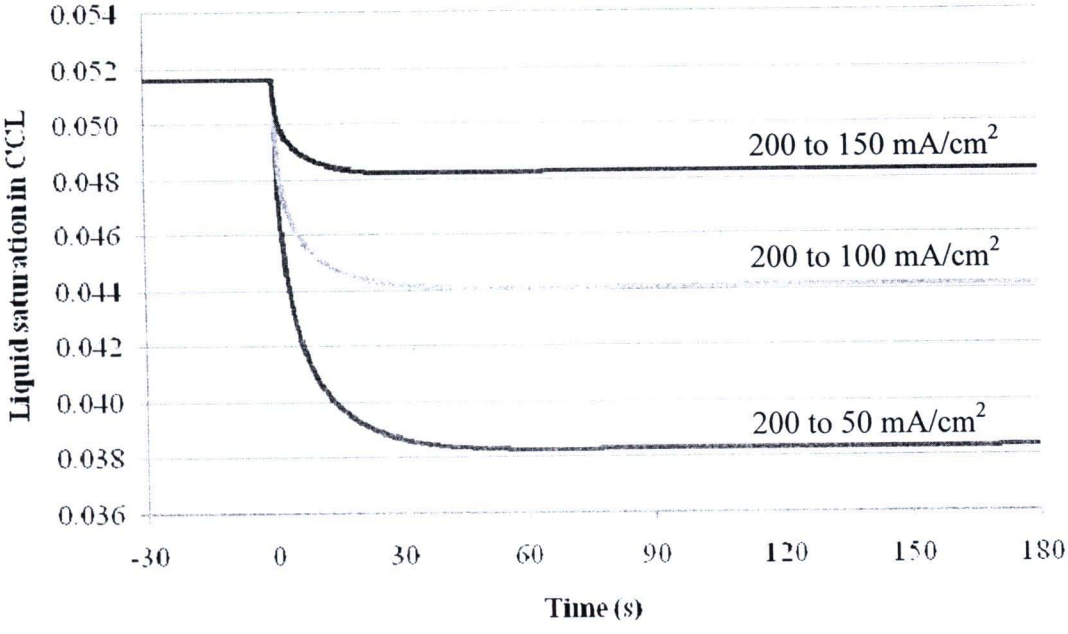

Figure 5.26 Dynamic behavior of the average liquid saturation in CCL

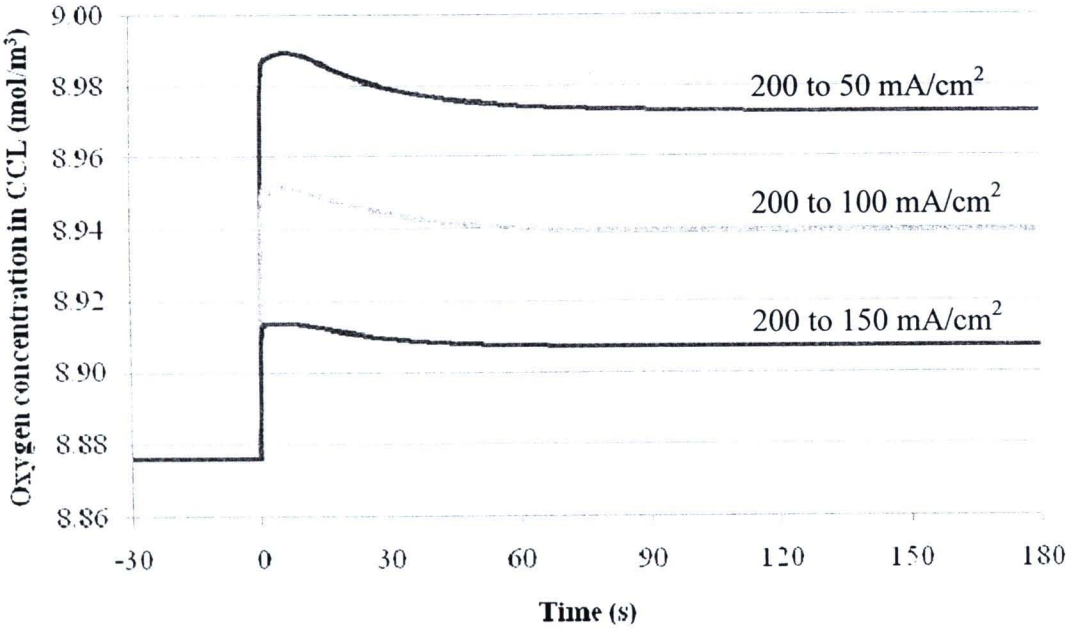

Figure 5.27 Dynamic behavior of the average oxygen concentration